Supporting Information

Synthesis of Bimetallic Pt-Pd Core-shell Nanocrystals and Their High Electrocatalytic Activity Modulated by Pd Shell Thickness

Yujing Li[1], Zhi Wei Wang[3], Chin-Yi Chiu[1], Lingyan Ruan[1], Wenbing Yang[1], Yang Yang[1,2], Richard E. Palmer[3], Yu Huang[1,2]

1. Department of Materials Science and Engineering, University of California, Los Angeles., Los Angeles, 90095, United States.

2. California Nanosystems Institute, University of California, Los Angeles., Los Angeles, 90095, United States.

3. Nanoscale Physics Research Laboratory, University of Birmingham, Edgbaston, Birmingham, B15 2TT, United Kingdom.

Email: yhuang@seas.ucla.edu

1. Multipod Pt NCs were synthesized and coated with Pd shell as shown in Fig. S1. The Pt core NCs (Fig. S1A) were obtained by using 1 mM K_2PtCl_4, 0.5 mM $NaBH_4$, and 25 µg/mL BP7A with the experimental procedure described in methods and Ref. 1. Fig S1(B-D) show the bimetallic NCs synthesized when refluxed at 92 ^oC for 60, 90, 120 minutes, respectively.
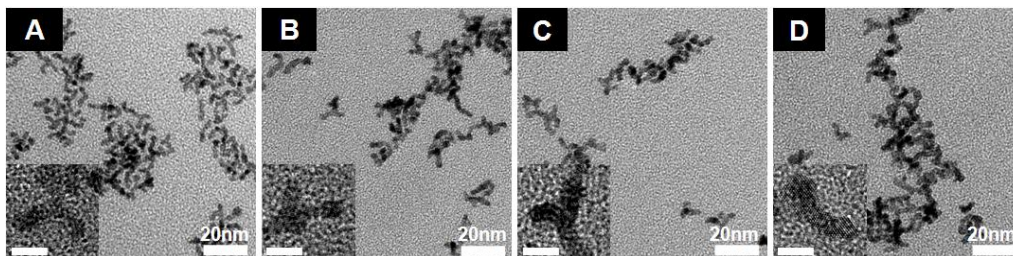

Figure S1. Pt-Pd core-shell NCs with long pod. (**A**) is preformed Pt core NCs with long pods, synthesized by using BP7A as capping agent. (**B-D**) are bimetallic Pt-Pd NCs with different Pd shell thicknesses by controlling the reaction time at 60, 90 and 120 min, respectively. Inset: HRTEM image of the NCs, scale bar: 5nm.

2. Pt NCs with shorter pods were also synthesized (with higher BP7A concentration) and coated with Pd shell of different thicknesses, as shown in Fig. S2. The Pt core NCs were synthesized with 1

mM K_2PtCl_4, 0.5 mM $NaBH_4$, and 100 µg/mL BP7A. Fig. S2(B-E) show the bimetallic NCs synthesized when refluxed at 92 °C for 30, 60, 90, 120 minutes, respectively. There is obvious change in morphology or dispersity with the formation of Pd shell.
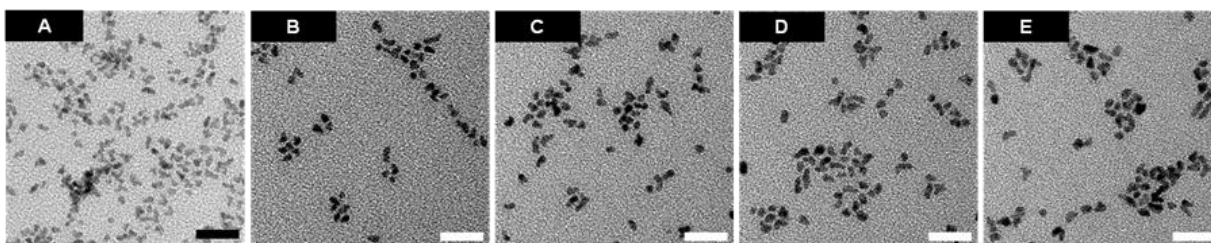

Figure S2. Pt-Pd core-shell NCs with short pod. (**A**) short pod Pt core NC. (**B-E**) Pt-Pd NCs synthesized with refluxing time of 30, 60, 90 and 120 minutes with 1mM Na_2PdCl_4 using (A) core NCs. Scale bars: 20 nm.

3. The core-shell structure is also characterized in high angle annular dark field scanning transmission electron microscopy (HAADF-STEM, on FEI TITAN STEM), energy-dispersive X-ray spectrometer (EDS, on FEI TITAN STEM), and electron energy loss spectroscopy (EELS, on aberration-corrected JEM2100F-Cs). Pt core NC, Pt-Pd core-shell NCs with Pd grown for 2 and 5 hours are shown in Fig. S3. Insets in Fig. S3 are line scanning profiles (by EDS) of Pt-L (blue) and Pd-L (red) along the radial direction of the pod. The line scanning profiles were displayed only in the regions close to the edge of the pod or the boundary between Pt and Pd for the purpose of showing how the Pd profile is evolving. The yellow axis indicates the scanning path and distance starting from 0. With thin Pd layer (Fig. S3B), Pd intensity (indicated by the axis in magenta) grows slowly. For thick Pd layer (Fig. S3C), obviously higher intensity of Pd at the shell region can be observed, indicating the existence of Pd shell. HAADF-STEM study confirms the core-shell structure and conformal growth of Pd shell on Pt core.
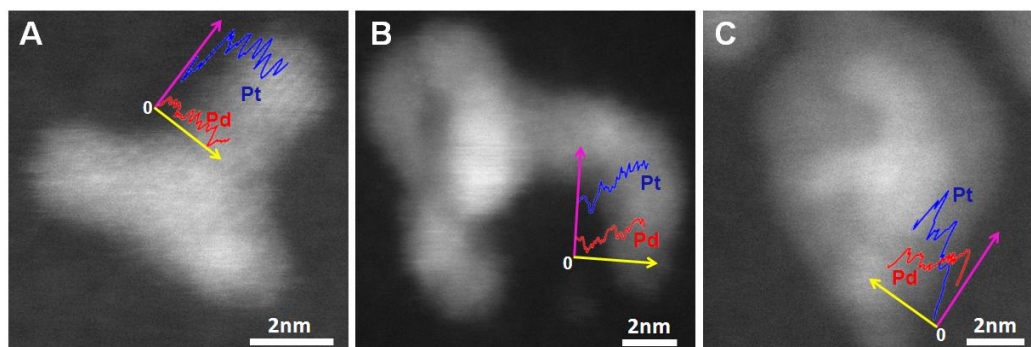

Figure S3. HAADF-STEM images of Pt-Pd core-shell NCs. (**A**) Pt multipod core NCs. (**B**) and (**C**) Pt-Pd NCs with Pd grown for 2 and 5 hours, respectively. **Insets** are EDS line scanning profiles of Pt-L and Pd-L along radial direction of pod. The blue curve is the Pt-L profile, and the red is Pd-L profile. Yellow axis indicates the scanning path and distance starting from 0, and magenta axis indicates the intensity (element counts).

4. XPS spectrum of Pt $4f_{5/2}$ and $4f_{7/2}$ for Pt core NCs is shown in Fig. S5, and XPS spectra of Pt $4f_{5/2}$,$4f_{7/2}$ and Pd $3d_{3/2}$, $3d_{5/2}$ for Pd/Pt=1/4 and 2/3 respectively are shown in Fig. S6.

XPS was employed to examine the surface composition of the core-shell NCs with Pd/Pt ratios of 1/4 and 2/3, respectively. Three deconvoluted peaks are used to fit both the Pt $4f_{5/2}$ and $4f_{7/2}$ peaks as shown in Fig. S4. The main contribution comes from the Pt(0), while the lowest contribution comes from the binding energy of the Pt-O bond. The Pt(2+) contribution may from the peptide residues on the surface where Pt atom may coordinate with amines,[1,2] although Pt-Cl bond on the surface might contribute as well due to the precursor ($PtCl_4^{2-}$) residues on the surface.[3] From the characteristic spectra of the Pd $3d_{3/2}$ and $3d_{5/2}$, three deconvoluted peaks were used to fit the spectra, one coming from the formation of Pd-Pt metallic bond, one from Pd(0) and the other from Pd-O bond.
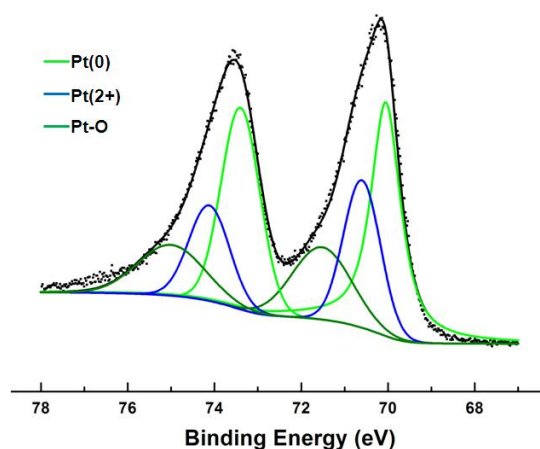

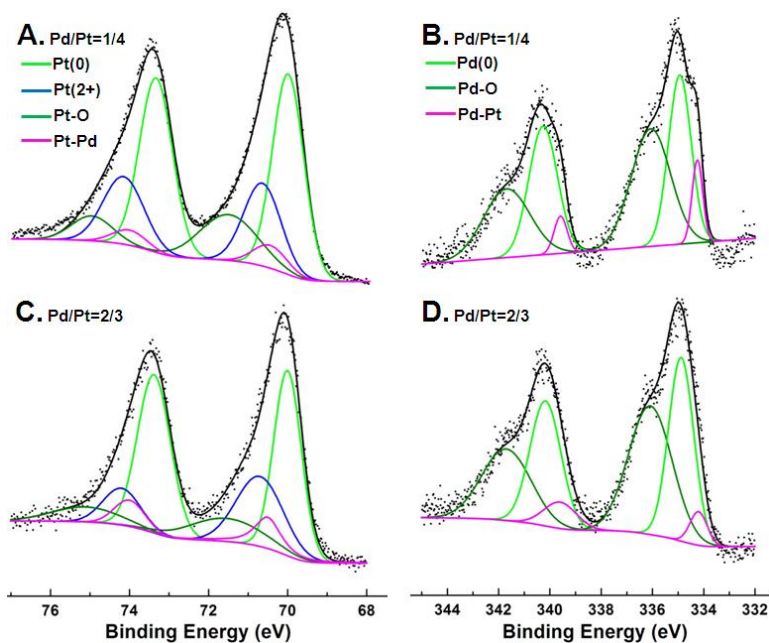**Figure S4.** XPS of Pt $4f_{5/2}$ and $4f_{7/2}$ for Pt core NCs.

Figure S5. Surface elemental characterization of Pd shell with XPS. (**A**) and (**C**) are XPS spectra of Pt $4f_{5/2}$ and $4f_{7/2}$ for Pt-Pd NCs with Pd/Pt 1/4 and 2/3. (**B**) and (**D**) are XPS spectra of Pd $3d_{3/2}$ and $3d_{5/2}$ for Pt-Pd NCs with Pd/Pt 1/4 and 2/3.

As the Pd/Pt ratio increases from 1/4 to 2/3, we can observe in Fig. S5A and C the decreased contribution from both Pt(2+) and Pt-O and the increased contribution from Pt-Pd bond, indicating Pd atom is replacing the amine residues and O on the surface and being deposited onto Pt. While in Fig. S5B and D, we observed the decreased contribution from Pd-Pt when Pd/Pt ratio increases from 1/4 to 2/3. This observation suggests that the Pd coating on Pt surface is incomplete at Pd/Pt 1/4, where the Pd-Pt bond carries more weight in the surface binding. Then with the completion of the Pd shell (greater than monolayer, when the Pd-Pt bonds reaches its maximum contribution) at Pd/Pt 2/3, Pd-Pd bond starts to populate the surface bonding and hence decrease the relative contribution from the Pd-Pt interface. This observation, together with the increased Pt-Pd contribution in Fig. S5A and C with increasing Pd deposition on Pt surface, confirms that the monolayer Pd shell formation happens between Pd/Pt 1/4 and 2/3. The XPS result also confirms that the surface of the bimetallic NCs is mainly in the oxide state.

5. Polarization curves and L-K plots.

The polarization curves and L-K plots of the control materials, including Pd and Pt black, Pt core NCs, as well as those of the bimetallic NCs with different Pd/Pt ratios including 1/3 and 2/3 are shown in Fig. S6. The curves were recorded in 0.1 M KOH at the rate of 10 mV/s and currents have been normalized by ECSA determined from hydrogen adsorption/desorption peak of cyclic voltammograms (CV) recorded in 0.5 M H_2SO_4 electrolyte.
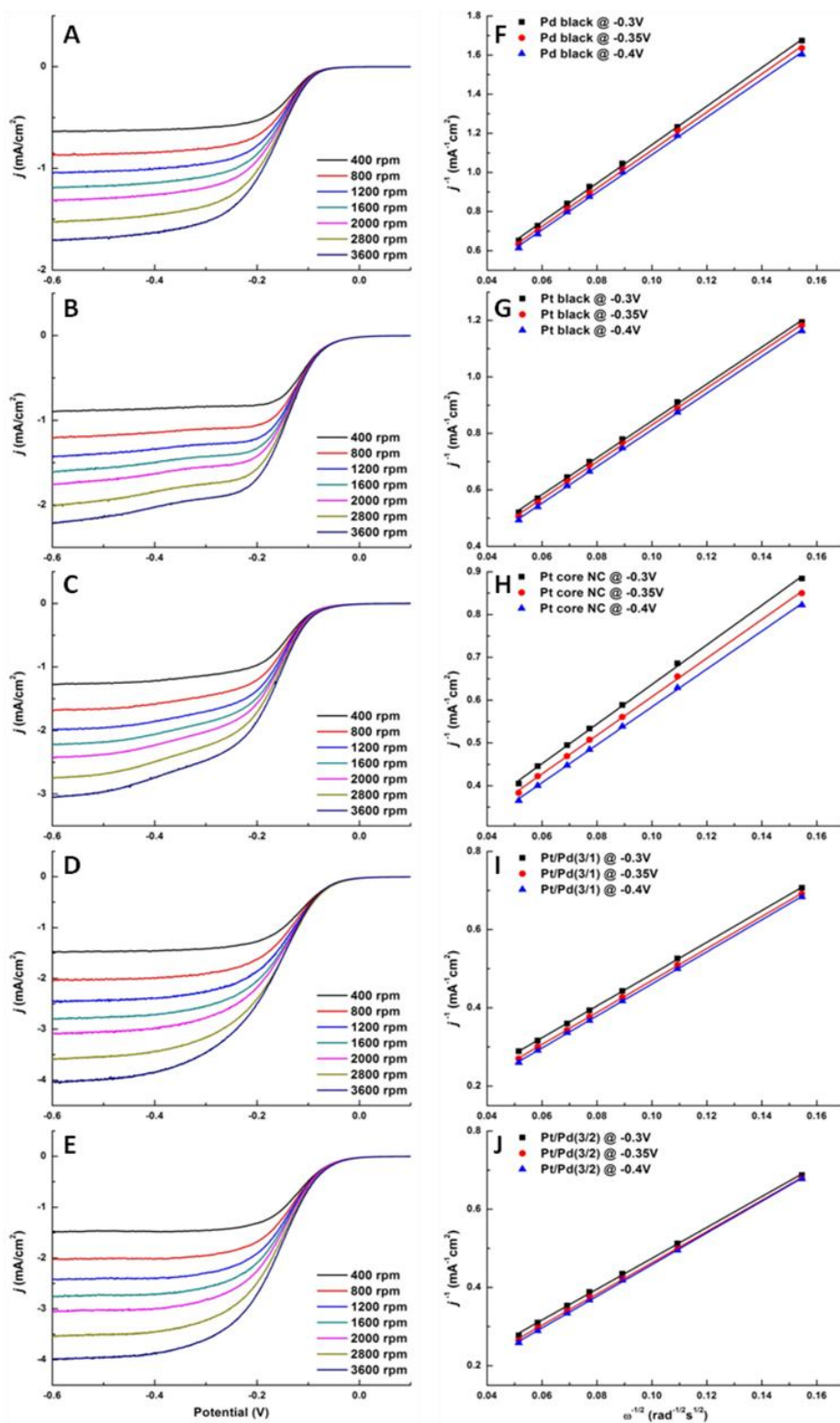
Figure S6. (**A-E**) are polarization curves of Pd black, Pt black, Pt core NCs, Pt-Pd NCs with Pd/Pt of 1/3 and 2/3 recorded at different rotating speeds. (**F-J**) are corresponding LK plots at -0.3, -0.35 and -0.4 V for above materials.
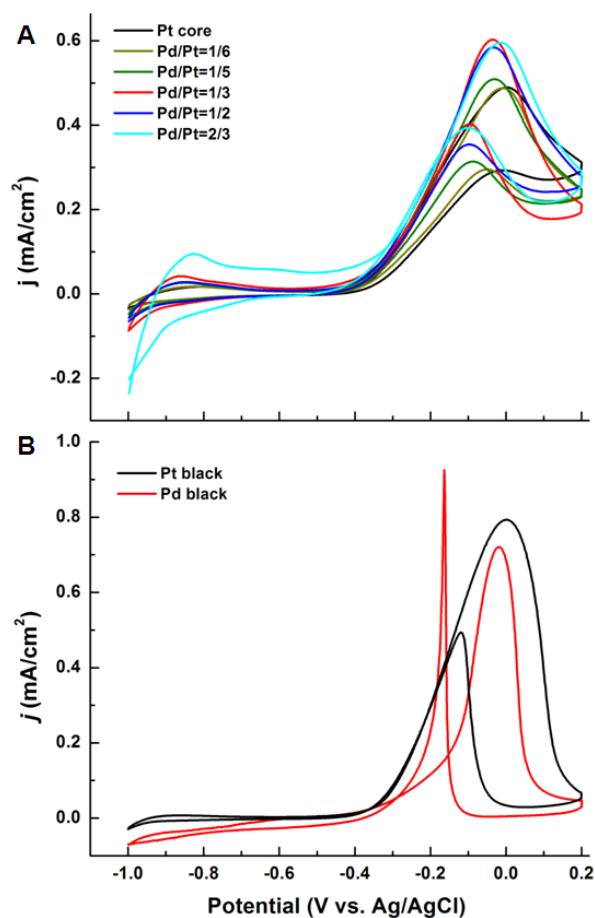
6. CV curves for methanol oxidation

Figure S7. Full CV curves for (**A**) Pt core and Pt-Pd NCs with Pd/Pt ratios of 1/6, 1/5, 1/3, 1/2, 2/3, and (**B**) Pt black and Pd black The CV curves were recorded in 0.1 M KOH electrolyte with 1 M methanol at the rate of 100 mV/s.

References

1. Li, Y. J.; Huang, Y., Morphology-Controlled Synthesis of Platinum Nanocrystals with Specific Peptides. *Advanced Materials* **2010**, *22* (17), 1921-1925.

2. Kumar, A.; Joshi, H. M.; Mandale, A. B.; Srivastava, R.; Adyanthaya, S. D.; Pasricha, R.; Sastry, M., Phase Transfer of Platinum Nanoparticles from Aqueous to Organic Solutions Using Fatty Amine Molecules. *Journal of Chemical Sciences* **2004**, *116* (5), 293-300.

3. Karhu, H.; Kalantar, A.; Vayrynen, I. J.; Salmi, T.; Murzin, D. Y., XPS Analysis of Chlorine Residues in Supported Pt and Pd Catalysts with Low Metal Loading. *Applied Catalysis a-General* **2003**, *247* (2), 283-294.